



Screen-printed flexible temperature sensor based on FG/CNT/PDMS composite with constant TCR

Linhui Wu¹ · Jun Qian¹ · Jinhua Peng¹ · Ke Wang¹ · Zhangming Liu¹ · Taolin Ma¹ · Yihua Zhou¹ · Gaofeng Wang¹ · Shuangli Ye¹

Received: 10 December 2018 / Accepted: 6 April 2019 / Published online: 11 April 2019
© Springer Science+Business Media, LLC, part of Springer Nature 2019

Abstract

This work presents the fabrication and characterization of a flexible temperature sensor based on the flake graphite (FG)/carbon nanotube (CNT)/polydimethylsiloxane (PDMS) composite. The sensor shows high temperature sensitivity and good linearity. The FG/CNT/PDMS temperature-sensitive films are prepared by the screen printing process. Superior printability of the FG/CNT/PDMS inks is demonstrated by means of rheology. Field emission scanning electron microscope investigation reveals an interpenetrating network structure between the FG and CNT. Moreover, thermal gravity analysis illustrates that the FG/CNT/PDMS temperature-sensitive films have a better thermal stability than that of PDMS blank control film. The temperature-dependent resistance behavior suggests that the temperature coefficient of resistance (TCR) value of the FG/CNT/PDMS films can be manipulated by the mass ratio of FG to CNT. When the mass ratio of FG to CNT is 4:1, the TCR is almost reproducible and maintained at the same level of 0.028 K^{-1} for repeated thermal cycles. These results indicate that the developed FG/CNT/PDMS composite has potential applications for the flexible temperature sensor.

1 Introduction

In the past decades, due to the rapid development and significant achievement of the Internet of Things [1], the advancements in developing and implementing flexible temperature sensors have demonstrated their importance and potential applications [2–5]. Meanwhile, along with innovations in both the material science and fabrication technology, flexible temperature sensor has been continuously matured. Typically, for the temperature-sensitive flexible sensor based on the polymer, conductive fillers have been widely used. However, for the PE, HDPE and PS Polyolefin with conductive fillers [6–9], the fabrication process requires higher heating temperature due to the high melting point of the polymer. In addition, the conductive polymer composites exhibit very weak resistance temperature sensitivity. These shortcomings have restricted the further industrial application and promotion of the conductive polymer composites. In order to save energy and increase temperature sensitivity, researchers are currently looking for new materials for replacement. The

organic PDMS can be a potential and effective alternative material to meet or optimize such requirements owing to its transparency, chemical inertness, simple in the fabrication process, excellent hydrophobic and permeability, especially superior thermal expansion performance [10, 11]. The electrically insulating PDMS can be converted into a conductive material by adding conductive materials like metal or metal complex compounds [12]. Niu et al. synthesized two conducting composites by mixing silver and carbon black into PDMS gel, respectively [13]. Experimental results showed that the threshold concentration for Ag-PDMS composite is very high (ca. 83 wt%). It should be pointed out that the more addition of fillers, the higher the cost, the worse the processing performance. At the same time, it is worth noting that patterning metallic specific uniform structure structures during the entire preparation process is a challenge due to the weak adhesion between the metal and PDMS as well as poor compatibility.

On the other hand, carbon materials filled PDMS-based conductive composites for temperature sensor have attracted increasing attention. Tsao et al. use PDMS as the matrix of the temperature-sensitive composites which is filled with different carbon conductive fillers such as carbon black, graphite powder, and carbon nanofiber, respectively [14]. Results indicate that graphite powder serves as the best

✉ Shuangli Ye
slye@whu.edu.cn

¹ School of Printing and Packaging, Wuhan University, Wuhan 430072, Hubei, People's Republic of China

conductive filler for the highest temperature sensitivity and better stability. Shih et al. fabricated a graphite-PDMS sensor by an automatic dispensing method. This temperature sensor has different applications according to the volume fraction of graphite [15]. The composite with low graphite powder concentration is suitable for on/off devices while high filling concentration is used for continuous temperature measurement. Bali et al. presented a fully inkjet-printed flexible temperature sensor based on carbon and PEDOT: PSS [16]. The Wheatstone bridge sensor shows good linearity and exhibits high temperature sensitivity. Irrespective of the filled carbon materials [17], semiconductors [18], and metals [19] in polymers as effective sensing component of the sensors, their temperature coefficient of resistance (TCR) cannot be maintained at the same level after every thermal cycle. Moreover, most of the composites work under a single mechanism, and their output performance presents irreversible and uncontrollable change once they undergo a thermal cycle. Therefore, these PDMS-based temperature sensors are seriously challenged in the practical applications of temperature measurement.

In this paper, we amply present the process for a low-cost and easy-fabrication flexible temperature sensor with the screen-printing technology, including the preparation of temperature-sensitive film and sensor electrodes. The printing feasibility of the FG/CNT/PDMS inks has been investigated. A temperature-sensitive film with a constant TCR value is obtained by designing the conductive fillers in the FG/CNT/PDMS composite, which shows a good performance in temperature sensitivity as well. At the end of the article, an understandable temperature sensing mechanism based on the micro-structure of the FG/CNT/PDMS composite is proposed.

2 Experimental and method

2.1 Materials

A SYLGARD® 184 elastomer kit is purchased from Dow Corning, USA. PDMS blank control with a good heat and electric insulation is fabricated by mixing the base and curing agent with a mass ratio of 10:1. Carbon materials including flake graphite (FG, Qingdao Yanhai Carbon Material Co., Ltd, grade HGP-2) and carbon Nanotube (CNT, Zhongshan Guoan Torch Development Co., Ltd, grade GA03-3) are used as conductive fillers. Cyclohexane used as dispersant is supplied by Sinopharm Chemical Reagent Co., Ltd. Protective layer-covered polyethylene terephthalate (PET) purchased from Max Electromechanical Hardware is used as flexible substrate material. Silver conductive paste is purchased from Loka Chemicals Laboratory (Germany). All chemical reagents are analytical purity and used without further processing.

2.2 Fabrication of temperature-sensitive ink and sensor

The preparation process of FG/CNT/PDMS temperature-sensitive ink and sensor is clearly illustrated in Fig. 1. Firstly, the colorless and transparent PDMS is accurately weighed by an electronic analytical balance, then mixed with cyclohexane followed by sonication in Scientz SB-5200 DTD Ultra Sonic Cleaner (90% amplitude; duration: 10 min). The mass of the cyclohexane is two times than that of total carbon materials. The function of cyclohexane is to reduce the agglomeration of carbon materials for the uniformity of the mixture, which is benefited from the miscibility between cyclohexane and

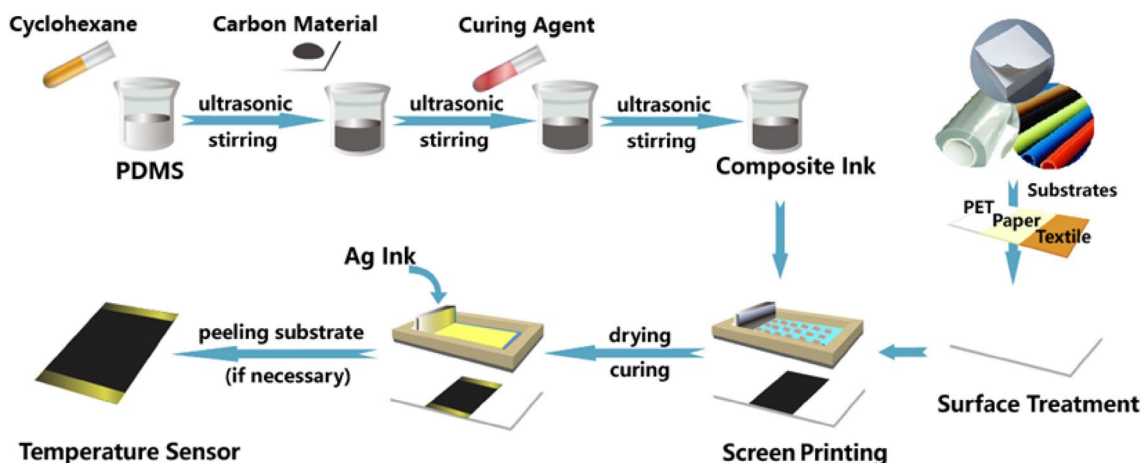


Fig. 1 The preparation process of temperature-sensitive ink and sensor

PDMS. Secondly, the mixtures are configured by changing the mass ratio of the FG to CNT (i.e., 5:1, 4:1, 3:1, 1:1, and only FG added), in which the total amount of carbon materials including FG and CNT keeps constant at 16 wt%. The FG/CNT mixture is uniformly distributed into above homogeneous dispersion followed by the mixing operations including the ultrasonic mixing and stirring for 30 min, respectively. After the mixing operations, there are no visible aggregation can be found. Thirdly, the PDMS curing agent is added into the above slurry-like mixture, and the mixing operations are performed again. The mass ratio of PDMS pre-polymer to curing agent is 10:1. Fourthly, the mixtures are placed in a vacuum chamber for 30 min to reduce bubbles and evaporate residual volatile cyclohexane. For comparison, a blank control without conductive filler is also fabricated using the same method. At last, the screen printing process is applied to fabricate the flexible temperature sensor including two steps of temperature-sensitive film printing and electrode printing. Theoretically, the prepared FG/CNT/PDMS ink can be printed on kinds of substrates including paper, textile, plastic, glass, etc. In this paper, a flexible temperature sensor printed on PET is demonstrated. The temperature-sensitive film is obtained with FG/CNT/PDMS ink printed by a screen plate of 40 meshes and an appropriate speed of 30 m/min, and then dried at 100 °C for 2 h. Subsequently, the conductive silver paste ink is overprinted to the two ends of the temperature-sensitive film to serve as stretchable electrodes, and then dried at 80 °C for 1 h to solidify the electrodes. For comparison, all temperature sensors are fabricated with the same procedure.

2.3 Characterization and measurement

The rheological behavior of the FG/CNT/PDMS ink is studied by Kinexus Pro+ rotational rheometer (Malvern, England). The shear viscosity test is performed with an specific shear rate increasing from 0.1 to 1000 s^{-1} , and the thixotropy is obtained through three-step shear rate testing, whose shear rate and test time are 0.1, 1000, 0.1 s^{-1} , and 60, 60, 120 s, respectively. The cross-sectional microstructure of the FG/CNT/PDMS temperature-sensitive films are investigated by field emission scanning electron microscopy (Zeiss Sigma, Carl Zeiss Jena, England) instrument operated at an acceleration voltage of 20 kV. The thermal gravimetric analysis is carried out on a TG and DTG system (Hitachi, Japan) with a heating rate of 15 °C/min in a nitrogen atmosphere from 30 to 800 °C. The sensitivity and stability of the fabricated flexible temperature sensor based on the FG/CNT/PDMS temperature-sensitive films are obtained by measuring the changes in resistance with multimeter (Agilent 34410A).

3 Results and discussion

3.1 Rheological property of FG/CNT/PDMS inks

The printing feasibility of the FG/CNT/PDMS inks is characterized by the rheology measurements. It can be found that the viscosity increases with the increasing concentration of CNT for the FG/CNT/PDMS ink with the constant carbon materials concentration at 16 wt%, as shown in Fig. 2a. Moreover, the viscosity decreases with the increasing of the shear rate, which is consistent with the properties of pseudo-plastic fluids. Particularly, as the shear rate increases, it can be seen that the viscosity reduces dramatically before

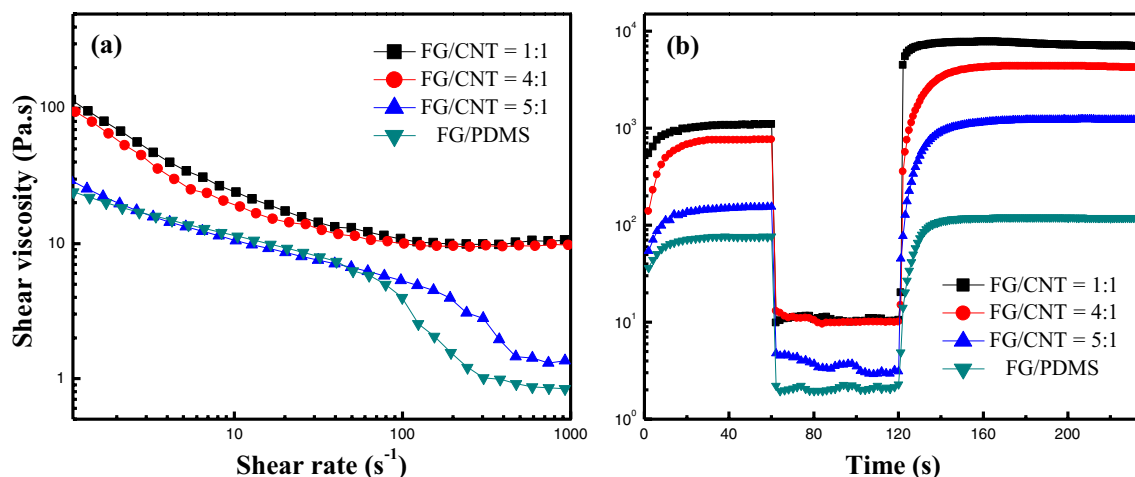


Fig. 2 Shear rate-dependent viscosity (a), time-dependent viscosity of the three-step shear rate test (b) for the FG/CNT/PDMS inks with the FG to CNT mass ratio of 1:1, 4:1, 5:1, and FG/PDMS ink, respectively

reaches the constant value for the FG/CNT/PDMS inks with lower CNT concentration. In contrast, the viscosity does not decrease significantly but tend to be stable for the FG/CNT/PDMS inks with higher CNT concentration. These results demonstrate that the stability of the microstructure can be enhanced by the mixed addition of the FG and CNT together into the PDMS matrix. The improved stability can be explained by the entanglement and interaction between FG and CNT [20]. The FG interacts with the linear CNT into a whole network structure after an ultrasonic mixing process. Therefore, at low shear rate, a portion of the entangled network structure can be quickly rebuilt, leading to the slowly decreasing viscosity. As the shear rate increases, there have two inconsistent phenomena resulting from the different mass ratio of the FG to CNT. For inks with low CNT content, the entangled network structure cannot be recovered after being damaged due to the interactions between FG and CNT is weak, leading to the dramatically reduction of the viscosity. Once the shear rate is large enough to destroy most of the entangled structures, then the viscosity value reaches a minimum and remains constant. For inks with high CNT content, the interaction between FG and CNT is enhanced. Even at a very high shear viscosity (1000 s^{-1}), part of destroyed interlaced network structure can still be recovered, so viscosity does not decrease significantly but tend to be stable.

On the other hand, time-dependent viscosity curves for the FG/CNT/PDMS ink with different mass ratio of FG to CNT are shown in Fig. 2b. When the shear rate changes from 0.1 to 1000 s^{-1} , the viscosity of all ink is reduced by two orders of magnitude. Viscosity increases rapidly when shear rate changes from 1000 to 0.1 s^{-1} . Compared to that of FG/PDMS ink, the reconstruction time is prolonged with the addition of CNT, revealing the stronger thixotropy, which can be due to the more complicated intercrossing network structure and physical interaction between FG and CNT. But there is an exception like the ink of FG/CNT = 1:1, which may be caused by the agglomeration of CNT, resulting in a reduced rebuild time and worse thixotropy. Therefore, these results indicate that FG/CNT/PDMS ink meets the two basic requirements for screen printing technology, i.e., good fluidity and thixotropy. Moreover, it illustrates that the mixed types of carbon materials can modify the micro-structure and the structure stability of ink.

3.2 The microstructure of FG/CNT/PDMS temperature-sensitive films

The cross-sectional surface dispersion pattern for the FG/CNT/PDMS temperature-sensitive films with different mass ratio of FG to CNT are characterized by the field emission scanning electron microscope (FESEM), as shown in Fig. 3. The inset shows a photomicrograph of 30,000 times

magnification at the same position. It can be found that the distribution of the CNT and FG is strongly dependent on the mass ratio of FG to CNT. Figure 3a shows the cross-sectional surface dispersion for the FG/CNT/PDMS film with 5:1 mass ratio of FG to CNT. It can be seen that most of CNT are located independently, and no obvious entanglement or cross network between the CNT and FG can be observed. However, when the mass ratio of FG to CNT is increased to 4:1 and 3:1, it can be seen that more and more CNT are deposited on the surface of FG, resulting in an interpenetrating network structure [21–23], as shown in Fig. 3b, c. Clusters induced by excess CNT are observed when the mass ratio of FG to CNT increasing to 1:1 [24, 25], as shown in Fig. 3d. Therefore, the FESEM results indicate that the distribution and homogeneity of the FG/CNT/PDMS temperature-sensitive film is significantly influenced by the mass ratio of FG to CNT, which can lead to the mass ratio-dependent physical properties.

3.3 Thermal gravimetric analysis of FG/CNT/PDMS films

The influence of the CNT content on the thermal properties of FG/CNT/PDMS film is investigated by the thermal gravimetric analysis (TGA). Figure 4a presents the thermal degradation behavior for the FG/CNT/PDMS films with different mass ratio of FG to CNT. Compared to that of PDMS blank control and CNT/PDMS films, it can be found that the onset temperatures of FG/CNT/PDMS films are significantly increased. On the other hand, it can be observed that the residue weight at $800 \text{ }^\circ\text{C}$ is far higher for the FG/CNT/PDMS films than that of FG/PDMS except for the 1:1 mass ratio of FG to CNT. The CNT/PDMS has lowest residue weight at $800 \text{ }^\circ\text{C}$, which might be attributed to the mass agglomeration of CNT [24]. Therefore, the TGA results indicate that FG/CNT/PDMS films have a better thermal stability than that of PDMS blank control. Figure 4b shows the derivative of the thermo-gravimetric profiles presenting the temperature where the maximum rate of structure damage occurs. T_d is defined as the temperature at which maximum weight loss is reached. The T_d value for PDMS blank control, CNT/PDMS, FG/PDMS and FG/CNT/PDMS films with different mass ratio of 5:1, 4:1, 3:1, and 1:1, are $512 \text{ }^\circ\text{C}$, $510 \text{ }^\circ\text{C}$, $533 \text{ }^\circ\text{C}$, $537 \text{ }^\circ\text{C}$, $552 \text{ }^\circ\text{C}$, $582 \text{ }^\circ\text{C}$, and $546 \text{ }^\circ\text{C}$, respectively. Obviously, the T_d value of FG/CNT/PDMS films are higher than that of PDMS blank control, CNT/PDMS and FG/PDMS films. Therefore, the DTG results indicate that the excellent thermal degradation property of FG/CNT/PDMS films, which may be caused by the interaction between FG and CNT. Such phenomenon has also been reported by Zhao et al. [26]. On the other hand, the T_d value of FG/CNT/PDMS films slightly rises with the increasing CNT content, which might be attributed to the improving structural

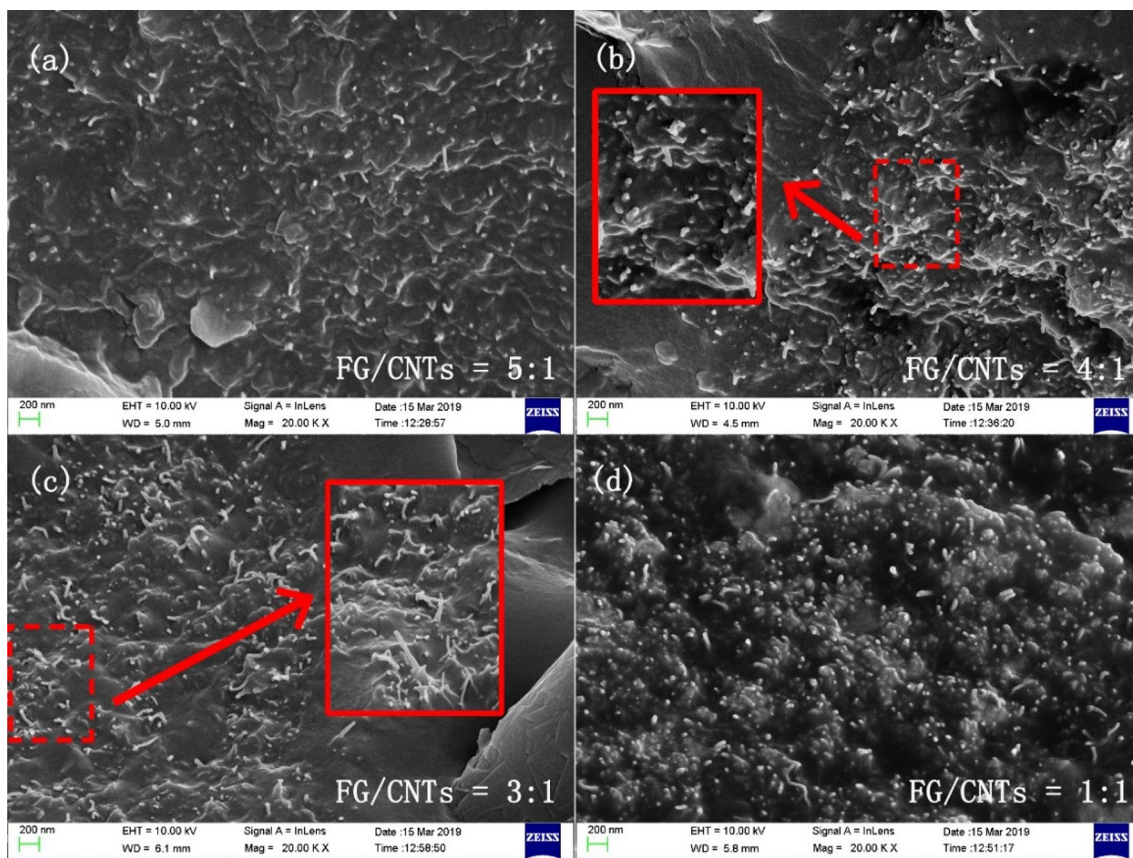


Fig. 3 The cross-sectional FESEM micrographs of FG/CNT/PDMS films with the mass ratio of FG to CNT are 5:1 (a), 4:1 (b), 3:1 (c), and 1:1 (d), respectively. The inset shows a micrograph of 30,000 times magnification at the same position

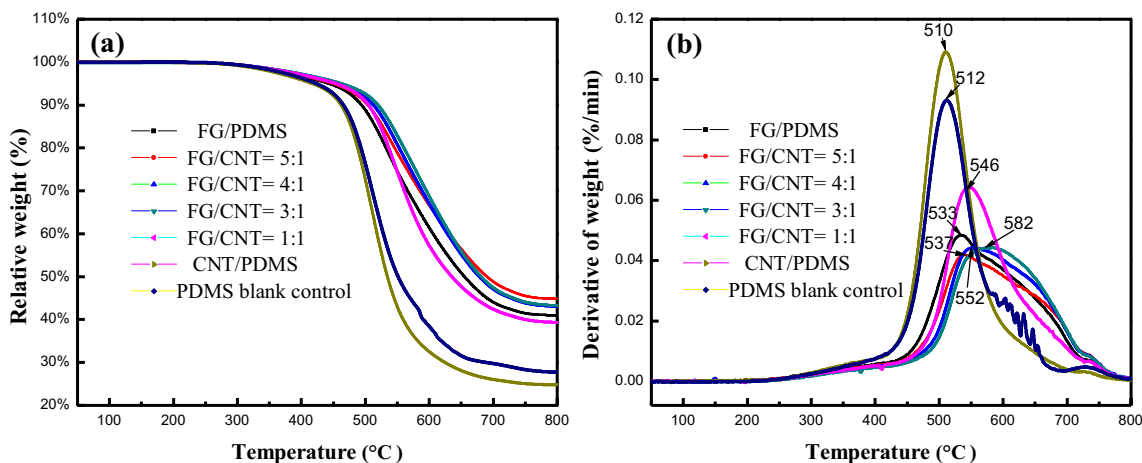


Fig. 4 TGA analysis plots (a), and DTG curves (b) for FG/PDMS films, FG/CNT/PDMS films with different mass ratio of FG to CNT (5:1, 4:1, 3:1, 1:1), CNT/PDMS films and PDMS blank control, respectively

strength by the synergistic effect of the intertwined network structure constructed between FG and CNT. The small T_d value for the films whose mass ratio of FG/CNT is 1:1 can be attributed to the abundant agglomeration of excess CNT [24]. These results illustrate that an excellent thermal

stability can be obtained for FG/CNT/PDMS film when the mass ratio of FG to CNT is 3:1 and 4:1, respectively. It has a good agreement with the FESEM results, which confirms the influences of the distribution and homogeneity of microstructure on the thermal properties.

3.4 Temperature coefficient of resistance

The comparison of the temperature-dependent resistance characterization of FG/PDMS temperature-sensitive films and CNT/PDMS temperature-sensitive films is shown in Fig. 5a, b, with mass fractions are 16 wt% and 8 wt%, respectively. For each thermal cycle measurement, at least three samples are tested and then averaged. It can be clearly seen that FG/

PDMS films and CNT/PDMS films have opposite temperature coefficient of resistance (TCR). The TCR is a vital parameter for many practical applications of temperature sensor which refers to the relative change in resistance when the temperature increases by one degree Celsius. TCR can be calculated by

$$\alpha = (\Delta R/R_0)/(T - T_0),$$

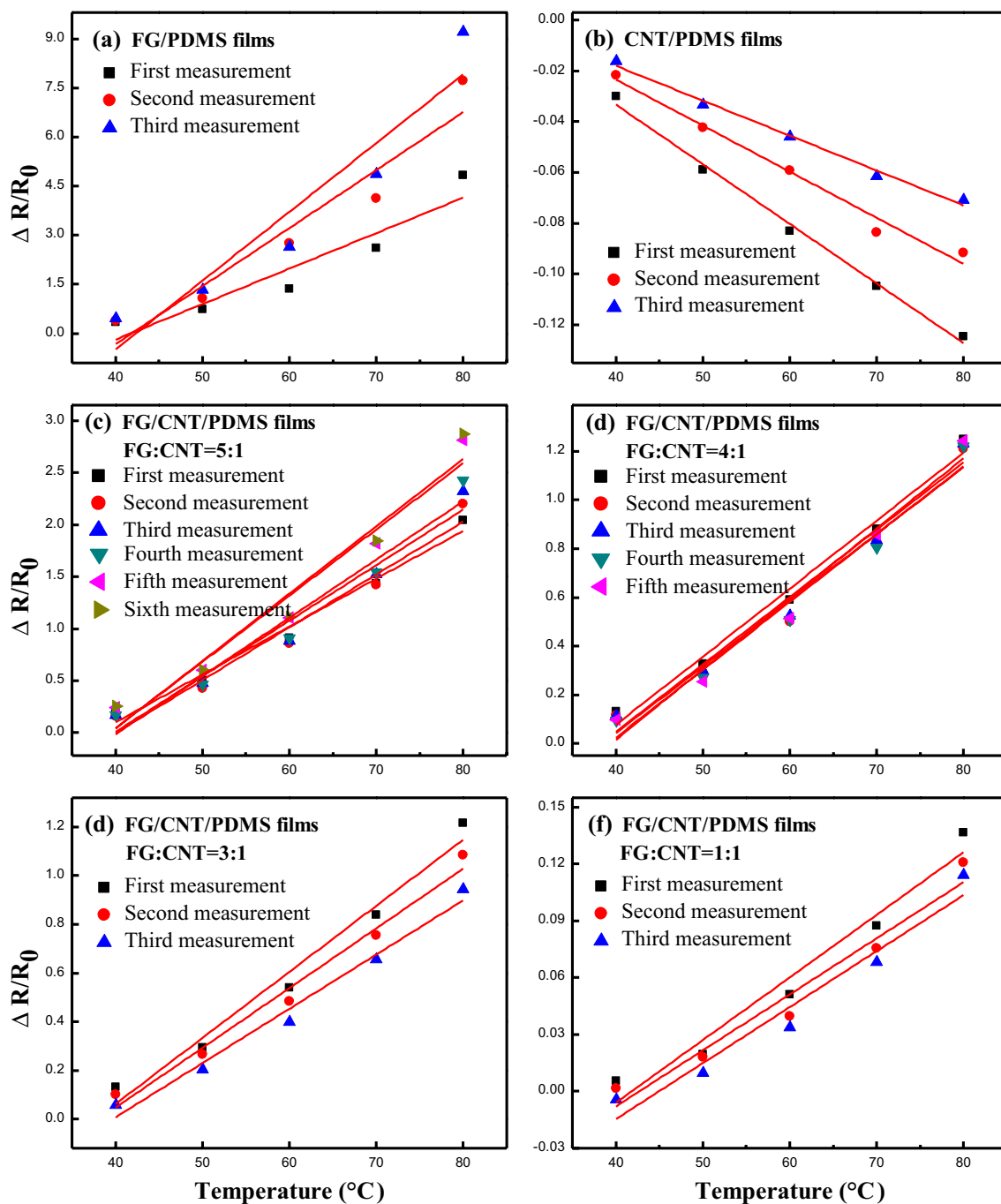


Fig. 5 Average resistance change of 16 wt% FG/PDMS film (a), 8 wt% CNT/PDMS film (b), and 16 wt% FG/CNT/PDMS films with FG/CNT=5:1 (c), FG/CNT=4:1 (d), FG/CNT=3:1 (e), and FG/CNT=1:1 (f) as a function of temperature, respectively

where α is the TCR. R_0 represents the resistance value measured in the initial temperature T_0 (30 °C) and ΔR is equal to $R - R_0$, respectively. As shown in the Fig. 5a, the FG/PDMS films show a positive TCR. Moreover, it can be found that the TCR value gets bigger after a complete thermal cycle, corresponding to 0.108 K^{-1} , 0.177 K^{-1} and 0.210 K^{-1} for the three thermal cycles, respectively. However, Fig. 5b shows that the CNT/PDMS films present a negative temperature coefficient of resistance. In contrast, the absolute value of TCR gets smaller after a complete thermal cycle, corresponding to 0.0023 K^{-1} , 0.0018 K^{-1} and 0.0015 K^{-1} for the three thermal cycles, respectively. It can be found that the absolute TCR of 16 wt% FG/PDMS films is one order of magnitude larger than that of 8 wt% CNT/PDMS films, as well as the fact that the absolute TCR of CNT/PDMS films decrease with increasing concentration of CNT [15], which indicates that FG/PDMS have a higher temperature sensitivity than that of CNT/PDMS. These results demonstrate that different carbon materials fillers have different effects on the TCR value of temperature-sensitive film and the change trend of TCR value.

The temperature-dependent resistance relative change ratio for FG/CNT/PDMS temperature-sensitive films is shown in Fig. 5c-f. It can be found that all the resistance increases with the increasing temperature, suggesting a positive TCR with high temperature sensitivity. Moreover, we can find that the TCR of all FG/CNT/PDMS films show good linearity, especially for the sample with a mass ratio of 4:1. However, the thermal stability is quite different for the FG/CNT/PDMS temperature-sensitive films with different mass ratio of FG to CNT. It can be seen that the TCR value for the 5:1 mass ratio of FG to CNT is 0.046 K^{-1} , 0.050 K^{-1} , 0.053 K^{-1} , 0.056 K^{-1} , 0.063 K^{-1} , and 0.064 K^{-1} for sixth

thermal measurements, respectively. In contrast, the TCR value keeps constantly at 0.028 K^{-1} for the FG/CNT/PDMS film with the 4:1 mass ratio of FG to CNT for five separated thermal measurement, they are 0.028 K^{-1} , 0.027 K^{-1} , 0.028 K^{-1} , 0.028 K^{-1} , and 0.028 K^{-1} , respectively. With the decreasing mass ratio of FG to CNT to 3:1, the TCR value turns to unstable again, presents 0.027 K^{-1} , 0.025 K^{-1} , and 0.022 K^{-1} for three thermal measurements, respectively. The unstable TCR value happens for the mass ratio of FG to CNT to 1:1 as well as shown in Fig. 5f, where the TCR value is 0.0033 K^{-1} , 0.0029 K^{-1} , and 0.0029 K^{-1} for three thermal measurements, respectively. These results indicate that the TCR value and stability of FG/CNT/PDMS films can be regulated by adjusting the mass ratio of FG to CNT. Moreover, the results illustrate that the FG/CNT/PDMS films with a 4:1 mass ratio of FG to CNT whose TCR value barely changes with temperature has a potential application in practical flexible temperature sensor.

3.5 The temperature sensing principle of temperature-sensitive films

A general effective contact theory is adopted to explain the temperature dependent resistance behaviors of FG/CNT/PDMS film. Figure 6a–c details the temperature sensitive mechanism for FG/PDMS film, CNT/PDMS film, and FG/CNT/PDMS film, respectively. From left to right, the distribution of the carbon materials is presented as a function of the initial temperature, medium temperature, higher temperature, and restore to initial temperature. The increasing temperature induces the expansion of PDMS, leading to the transformation of carbon conductive pathways and resistance change. Figure 6a details the

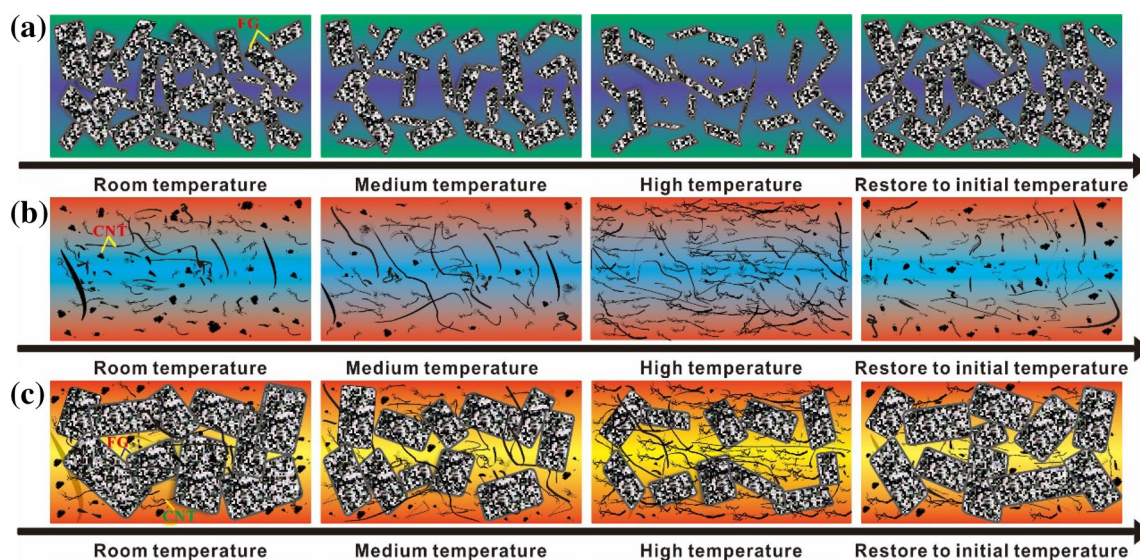


Fig. 6 Illustration of the temperature sensitive mechanism for FG/PDMS film (a), CNT/PDMS film (b), FG/CNT/PDMS film (c), respectively

principle for pure FG/PDMS temperature-sensitive film. FG is disorderly mixed and distributed homogeneously in PDMS at initial temperature status. With increasing temperature, the disorderly stacked FG spread out slowly, and their spacing is getting bigger and bigger induced by the thermal expansion of PDMS matrix. The effective conductive pathways decrease with the decreasing contacted FG, leading to an increasing resistance and positive TCR. Meanwhile, the movement of the FG can reduce the agglomeration and induce the anisotropy distribution of FG after the thermal cycle. The anisotropy distribution of FG causes more pronounced relative resistance change and enhanced temperature sensitivity, leading to the increasing TCR value with thermal cycle. Simultaneously, Fig. 6b details the temperature-dependent distribution of the carbon materials for CNT/PDMS temperature-sensitive film. At initial temperature status, CNT is highly curled and disorderly distributes in PDMS matrix. With increasing temperature, most of highly twisted CNT fully stretch into lines benefit from the thermodynamic expansion of PDMS, leading to the increasing of conductive pathways and the reduced resistance value. Therefore, CNT/PDMS temperature-sensitive film shows a negative TCR. Meanwhile, the stretched CNT cannot return to their entangled status after the thermal cycle, leading to the decreasing amount of twisted CNT. Therefore, the relative resistance change is weakened every measurement one by one, corresponding to the weakened temperature sensitivity and decreasing absolute value of TCR after every thermal cycle.

For FG/CNT/PDMS film, the picture becomes more complicated, as shown in Fig. 6c. FG and CNT are disorderly mixed together in PDMS at initial temperature status. With increasing temperature, due to the fact that the temperature sensitivity of FGs is much higher than that of CNT, which dominates the temperature-dependent resistance behavior. Consequently, all FG/CNT/PDMS films present a positive TCR. On the other hand, the CNT contribute to the negative TCR with increasing temperature, which plays an important role in total TCR as well. For all FG/CNT/PDMS films, both of FG and CNT have impacts on TCR. The former tends to increase the TCR value of temperature-sensitive films, the latter is the opposite. Moreover, the rheology and TGA measurements confirm the existing physical interaction between FG and CNT fillers, which can influence the distribution of the FG and CNT. Therefore, the dynamic density of the conductive pathways can be tuned by the mass ratio of the FG and CNT fillers. For an appropriate mass ratio of FG to CNT such as 4:1, a thermo-elastic density of conductive pathways can be achieved for the repeated thermal cycle, leading to the constant TCR value.

4 Conclusions

A flexible temperature sensor consisting of FG/CNT/PDMS temperature-sensitive film, silver paste electrode, and flexible PET substrate has successfully fabricated by the screen printing technology, which has high temperature sensitivity and stability. The FG/CNT/PDMS inks show good shear thinning properties and thixotropy properties. The FESEM result reveals the interpenetrating network structures of FG/CNT/PDMS temperature-sensitive films. Furthermore, the TGA indicates that FG/CNT/PDMS temperature-sensitive films have a better thermal stability than that of PDMS blank control, which can be due to the cross-interpenetrating network structure. The temperature-dependent resistance behavior demonstrates that the TCR of the FG/CNT/PDMS films can be manipulated by the mass ratio of FG to CNT. The dynamic density of the conductive pathways is determined by the integrated effects of positive TCR, negative TCR and the interaction between the conductive fillers. When the mass ratio of FG to CNT is close to 4:1, the TCR value is almost maintained at the same level of 0.028 K^{-1} . In a word, this work illustrates that a low-cost flexible temperature sensor based on the FG/CNT/PDMS composites with high temperature sensitivity and stability can be realized by tuning the mass ratio of FG to CNT conductive fillers.

Acknowledgments The authors gratefully appreciate financial support offered by the National Natural Science Foundation of China (Grant Nos. 51371129 and 11174226).

References

1. L. Atzori, A. Iera, G. Morabito, The internet of things: a survey. *Comput. Netw.* **54**, 2787–2805 (2010)
2. S. Harada, K. Kanao, Y. Yamamoto, T. Arie, S. Akita, K. Takei, Fully printed flexible fingerprint-like three-axis tactile and slip force and temperature sensors for artificial skin. *ACS Nano* **8**, 12851–12857 (2014)
3. S.G. Yoon, S.T. Chang, Microfluidic capacitive sensors with ionic liquid electrodes and CNT/PDMS nanocomposites for simultaneous sensing of pressure and temperature. *J. Mater. Chem. C* **5**, 1910–1919 (2017)
4. G. Rosace, V. Trovato, C. Colleoni, M. Caldara, V. Re, M. Brucale, M.R. Plutino, Structural and morphological characterizations of MWCNTs hybrid coating onto cotton fabric as potential humidity and temperature wearable sensor. *Sens. Actuators B. Chem.* **252**, 428–439 (2017)
5. W. Honda, S. Harada, T. Arie, S. Akita, K. Takei, Wearable, human-interactive, health-monitoring, wireless devices fabricated by macroscale printing techniques. *Adv. Func. Mater.* **24**, 3299–3304 (2014)
6. G. Yang, R. Teng, P. Xiao, Electrical properties of crosslinked polyethylene/carbon black switching composites as a function of morphology and structure of the carbon black. *Polym. Compos.* **18**, 477–483 (1997)

7. S.H. Foulger, Reduced percolation thresholds of immiscible conductive blends. *J. Polym. Sci. Pol. Phys.* **37**, 1899–1910 (1999)
8. G.J. Lee, K.D. Suh, S.S. Im, Study of electrical phenomena in carbon black-filled HDPE composite. *Polym. Eng. Sci.* **38**, 471–477 (1998)
9. Z. Zheng, W. Li, H. Sun, Z. Cheng, J. Yan, H. Wang, X. Cui, Preparation and characterization of polystyrene/modified carbon black composite beads via in situ suspension polymerization. *Polym. Compos.* **34**, 1110–1118 (2013)
10. C.S. Park, K.I. Joo, S.W. Kang, H.R. Kim, A PDMS-coated optical fiber Bragg grating sensor for enhancing temperature sensitivity. *J. Opt. Soc. Korea* **15**, 329–334 (2011)
11. J.M. Engel, J. Chen, D. Bullen, C. Liu, Polyurethane Rubber as a MEMS Material: Characterization and Demonstration of an All-Polymer Two-Axis Artificial Hair Cell Flow Sensor, in *18th IEEE International Conference on Micro Electro Mechanical Systems*, vol. **2005** (IEEE, Miami Beach, FL, USA, 2005), pp. 279–282. <https://doi.org/10.1109/memsys.2005.1453921>
12. K.S. Lim, W.J. Chang, Y.M. Koo, R. Bashir, Reliable fabrication method of transferable micron scale metal pattern for poly(dimethylsiloxane) metallization. *Lab Chip* **6**, 578–580 (2006)
13. X.Z. Niu, S.L. Peng, L.Y. Liu, W.J. Wen, P. Sheng, Characterizing and patterning of PDMS-based conducting composites. *Adv. Mater.* **19**, 2682–2686 (2007)
14. L.C. Tsao, M.Y. Cheng, I.L. Chen, W.P. Shih, Y.J. Yang, F.Y. Chang, S.H. Chang, Flexible Temperature Sensor Array Using Electro-Resistive Polymer Forhumanoid Artificial Skin, in *TRANSDUCERS 2007–2007 International Solid-State Sensors, Actuators and Microsystems Conference*, vol. **1** (IEEE, Lyon, France, 2007), pp. 2287–2290. <https://doi.org/10.1109/senso.2007.4300626>
15. W.P. Shih, L.C. Tsao, C.W. Lee, M.Y. Cheng, C. Chang, Y.J. Yang, K.C. Fan, Flexible temperature sensor array based on a graphite-polydimethylsiloxane composite. *Sensors (Basel)* **10**, 3597–3610 (2010)
16. C. Bali, A. Brandlmaier, A. Ganster, O. Raab, J. Zapf, A. Hübler, Fully inkjet-printed flexible temperature sensors based on carbon and PEDOT: PSS1. *Mater. Today Proc.* **3**, 739–745 (2016)
17. B. Davaji, H.D. Cho, M. Malakoutian, J.K. Lee, G. Panin, T.W. Kang, C.H. Lee, A patterned single layer graphene resistance temperature sensor. *Sci. Rep.* **7**, 8811 (2017)
18. T. Someya, Y. Kato, T. Sekitani, S. Iba, Y. Noguchi, Y. Murase, T. Sakurai, Conformable, flexible, large-area networks of pressure and thermal sensors with organic transistor active matrices. *P. Natl. Acad. Sci. USA* **102**, 12321–12325 (2005)
19. J. Jeon, H.B.R. Lee, Z. Bao, Flexible wireless temperature sensors based on Ni microparticle-filled binary polymer composites. *Adv. Mater.* **25**, 850–855 (2013)
20. C. Phillips, A. Al-Ahmadi, S.J. Potts, T. Claypole, D. Deganello, The effect of graphite and carbon black ratios on conductive ink performance. *J. Mater. Sci.* **52**, 9520–9530 (2017)
21. K.T.S. Kong, M. Mariatti, A.A. Rashid, J.J.C. Busfield, Enhanced conductivity behavior of polydimethylsiloxane (PDMS) hybrid composites containing exfoliated graphite nanoplatelets and carbon nanotubes. *Composites B* **58**, 457–462 (2014)
22. S.Y. Yang, W.N. Lin, Y.L. Huang, H.W. Tien, J.Y. Wang, C.C.M. Ma, S.M. Li, Y.S. Wang, Synergetic effects of graphene platelets and carbon nanotubes on the mechanical and thermal properties of epoxy composites. *Carbon* **49**, 793–803 (2011)
23. S. Kumar, L.L. Sun, S. Caceres, B. Li, W. Wood, A. Perugini, R.G. Maguire, W.H. Zhong, Dynamic synergy of graphitic nanoplatelets and multi-walled carbon nanotubes in polyetherimide nanocomposites. *Nanotechnology* **21**, 105702 (2010)
24. M. Norkhairunnisa, A. Azizan, M. Mariatti, H. Ismail, L.C. Sim, Thermal stability and electrical behavior of polydimethylsiloxane nanocomposites with carbon nanotubes and carbon black fillers. *J. Mater. Sci.* **46**(8), 903–910 (2012)
25. J.Y. Oh, G.H. Jun, S. Jin, H.J. Ryu, S.H. Hong, Enhanced electrical networks of stretchable conductors with small fraction of carbon nanotube/graphene hybrid fillers. *ACS Appl. Mater. Interfaces* **8**, 3319–3325 (2016)
26. Y.H. Zhao, Y.F. Zhang, Z.K. Wu, S.L. Bai, Synergic enhancement of thermal properties of polymer composites by graphene foam and carbon black. *Composites B* **84**, 52–58 (2016)

Publisher's Note Springer Nature remains neutral with regard to jurisdictional claims in published maps and institutional affiliations.